Estimating Sea-Level Extremes Under Conditions of Uncertain Sea-Level Rise

John Hunter
Antarctic Climate & Ecosystems Cooperative Research Centre, Private Bag 80, Hobart, Tasmania 7001, Australia

July 4, 2009

Abstract. Estimation of expected extremes, using combinations of observations and model simulations, is common practice. Many techniques assume that the background statistics are stationary and that the resulting estimates may be used satisfactorily for any time in the future. We are now however in a period of climate change, during which both average values and statistical distributions may change in time. The situation is further complicated by the considerable uncertainty which accompanies the projections of such future change. Any useful technique for the assessment of future risk should combine our knowledge of the present, our best estimate of how the world will change, and the uncertainty in both. A method of combining observations of present sea-level extremes with the (uncertain) projections of sea-level rise during the 21st century is described, using Australian data as an example. The technique makes the assumption that the change of flooding extremes during the 21st century will be dominated by the rise in mean sea level and that the effect of changes in the variability about the mean will be relatively small. The results give engineers, planners and policymakers a way of estimating the probability that a given sea level will be exceeded during any prescribed period during the present century.

1. Introduction

We are now living in a world in which the climate is being substantially modified by human activity (IPCC, 2007a). These changes are leading to a wide range of impacts, just one of which is a rise in sea level at a sustained rate which has not been experienced for at least 5,000 years (Church et al., 2008, Fig. 1 of that paper).

Beginning at the end of the 19th century, an increase in the concentration of greenhouse gases in the atmosphere, caused primarily by anthropogenic emissions, contributed to a warming of the climate. The

rise in global temperature during the latter half of the 20th century and beyond was dominated by the effect of these anthropogenic greenhouse gases, over other influences, such as solar activity. From 1850-1899 to 2001-2005, global-average surface temperature increased by about 0.76°C (IPCC, 2007a), leading to warming of the oceans and melting of ice on land (Lemke et al., 2007; Bindoff et al., 2007). Church and White (2006) used a combination of tide-gauge records and satellite-altimeter data to reconstruct sea level from 1870 to 2001, showing a global-average rise of about 0.17 metres during the 20th century. Their reconstruction also suggests an acceleration of sea level from around zero rate of rise in 1820 to a rate of about 3 mm y^{-1} over the past decade. Other reconstructions, using only tide-gauge data (Holgate and Woodworth, 2004; Jevrejeva et al., 2006; Woodworth et al., 2008), have indicated similar rates of rise during the 20th century.

Section 2 describes the IPCC projections of global-average sea-level rise and Section 3 summarises the coastal impacts of this rise. Section 4 introduces some common definitions related to extreme value theory. Section 5 presents a method of estimating future exceedance probabilities for any period during the 21st century, Section 6 shows examples of applying this method to two Australian ports (Fremantle and Fort Denison, Sydney) and Section 7 provides a summary. Appendix A proposes time series of sea level rise for the 21st century and Appendix B provides the mathematical background to Section 5.

2. Projections of Global-Average Sea-Level Rise

Computer modelling has been used to provide projections of the future climate over time scales of centuries. Two inherent uncertainties are involved. The first (the 'scenario uncertainty') arises from the fact that the future social, economic and technological development of the world, and the consequent greenhouse-gas emissions, are poorly known. A range of plausible futures, or scenarios, have been used to describe the way in which emissions may change in the future. The second uncertainty (the 'model uncertainty') is related to shortcomings in the present knowledge of the science of climate change, partly due to fact that we do not know exactly the present climate state (the 'initial conditions'), and partly due to the fact that no model gives a perfect representation of the real world. The IPCC Fourth Assessment Report ('AR4') provided projections of sea-level rise at 2095 relative to 1990 (strictly, the difference between the average sea level over 2090-2099 and over 1980-1999; Meehl et al., 2007). The rise projected by the models for this period was 0.18 to 0.59 m, for a range of scenarios covering B1

(low emission) to A1FI (high emission), and including an uncertainty estimate based on the range of projections from the different models. The IPCC also recommended that an additional contribution of up to 0.2 m should be added to the upper limits of the projections to account for processes involving land ice in Greenland and Antarctica that are not fully included in the models; it should be noted that the AR4 adds the caveat that 'larger values cannot be excluded' (IPCC, 2007b). The resultant upper limit of the A1FI projection at 2095 is in good agreement with the similar projection from the Third Assessment Report ('TAR'; Church et al., 2001). The lower limit for B1 is roughly 0.1 m higher for the AR4 than for the TAR. In summary, the range of projected sea level at 2095 is 0.18 metres to 0.79 metres, relative to 1990.

Unfortunately, unlike the TAR, the AR4 only provided numerical projections for 2095 and not throughout the 21st century. Appendix A provides tables of minimum and maximum projections at decadal resolution, based on fitting the decadal time series from the TAR to the AR4 projections at 2095. These tables form the basis of sea-level rise projections used in the present paper. They are shown graphically in Fig. 1.

The projections of the AR4 require some qualification. Even though the AR4 represents an extensive assessment of the state of climate science at the present time, some scientists have suggested that the sea-level projections may have been underestimated. Rahmstorf (2007) (and later Horton et al. (2008) and Grinsted et al. (2009)) used the relationship between historical temperature and sea level to project sea level into the 21st century based on the TAR temperature projections (which are considered to be more reliable than the modelled sea-level projections). Rahmstorf's results suggested a rise of 0.5 to 1.4 metres at 2100 relative to 1990, but models of this simple type have attracted some controversy (e.g. Holgate et al., 2007; Schmith et al., 2007). Probably the most extreme projection comes from James Hansen, who has suggested that a rise of 5 metres over the 21st century is not implausible (Hansen, 2007). Rahmstorf et al. (2007) showed that, since 1990, both global temperature and global sea level have been tracking near the upper limit of the projections, again suggesting that the model projections may be underestimates. However, Pfeffer et al. (2008) considered glaciological constraints and concluded that an increase of more than 2 metres over the 21st century is physically untenable and an increase of 0.8 metres is more plausible. Finally, Raupach et al. (2007) and Canadell et al. (2007) have shown that global greenhouse-gas emissions are now tracking close to the (high-impact) A1FI scenario, and that the world is not yet following any reasonable

mitigation pathway. Therefore, it seems reasonable to view the higher end of the AR4 projections as very plausible.

3. Impacts of Future Sea-Level Rise

The rise in sea level is being felt, and will be felt, through an increased frequency of flooding events (the subject of this paper) and coastal erosion leading to substantial changes to the bathymetry and topography of soft coastal margins (e.g. sandy shorelines).

The results and techniques presented in this paper relate to the increase in the frequency of extremes caused by a rise in mean sea-level and *not* due to any additional increase in extremes *relative to* mean sea level, caused for example by more frequent and intense storminess. However, present evidence (Bindoff et al., 2007, Woodworth and Blackman, 2004) suggests that the rise in mean sea level is generally the dominant cause of the observed increase in the frequency of extreme events (i.e. that the statistics of the effect of storminess on sea level is approximately stationary).

4. Some Definitions

An extreme event is defined by a certain value (in this case, the water level) exceeding a given threshold. The frequency of extreme events is commonly described by the *average recurrence interval* or ARI (R), or by the *exceedance probability* (E) for a given period (T). The ARI is the average period between extreme events (observed over a long period with many events) while the exceedance probability is the probability of at least one exceedance event happening during the period T. They are related by (e.g. Pugh, 1996)

$$E = 1 - \exp(-T/R) \tag{1}$$

which involves the assumption (made throughout this paper) that exceedance events are independent (the occurrence of exceedance events therefore following a Poisson distribution).

The ARI is effectively synonymous with the *return period*, although the latter term is sometimes defined (e.g. Coles, 2001, p. 49) as the reciprocal of the *annual exceedance probability* (AEP; the exceedance probability for a period (T) of one year), which only asymptotes to the ARI as $T/R \rightarrow 0$. Use of the term 'ARI', which is unambiguous, is therefore preferred. The ARI is often estimated from the AEP using Eq. 1 with $T = 1$ year.

The exceedance probability for a range of threshold values defines an *exceedance distribution* for the given period, T. The first derivative of the exceedance distribution relative to the threshold value is simply the *frequency distribution* of the maxima for the period, T.

If the exceedance probabilities, E_1 and E_2, are known for any two periods, T_1 and T_2, then the exceedance probability, E_3, over the combined period $(T_1 + T_2)$ is given by

$$(1 - E_3) = (1 - E_1)(1 - E_2) \qquad (2)$$

and if the statistics remain stationary over the two periods then

$$(1 - E_3) = (1 - E_1)^{T_3/T_1} = (1 - E_2)^{T_3/T_2} \qquad (3)$$

which is consistent with Eq. 1 and again relies on the assumption that events are independent.

This paper describes a method of estimating the exceedance distribution for an extended period, taking into account sea-level rise during that period and its inherent uncertainty. This period would generally be associated with the life of a coastal asset, such as a building or other infrastructure; it is here termed the *asset period*.

When sea level and its variability are taken into account, planners and policymakers define levels below which activities such as building or road construction should not occur. Such a level is here termed the *planning level*.

5. The Method

The present statistics of extreme sea levels may be combined with projections of the rise in mean sea level (and their associated uncertainties), in order to provide estimates of the statistics of future extremes. Again, this analysis estimates the contribution to changes in the extremes caused by the rise in mean sea level rather than by any change in the variability. The technique to be presented is described in detail in Appendix B and will only be summarised here.

Time series of projected sea-level for this century were calculated as described in Section 2 and Appendix A. The IPCC projections have been traditionally related to a base year of 1990 while, in this paper, 2000 was used as the base year. Projections for year Y relative to 2000 levels were derived by subtracting the values in Tables I and II (Appendix A) for 2000 from the corresponding values for year Y (this approach is correct if the uncertainty is proportional to the time elapsed from the base year - a reasonable approximation during the early part of

the 21st century). At this stage, the projections were adjusted in order
to provide an estimate of *relative* sea-level rise (i.e. the sea-level rise
relative to the local land surface), by applying an appropriate (small)
adjustment for vertical land motion (an Australian-average value of
-0.3 mm y^{-1} due to land uplift; Lambeck, 2002). No other adjustment
was applied for regional variations in sea-level rise.

Future sea-level extremes, and their statistics, depend on the tra-
jectory that mean sea level will follow. Tables I and II in Appendix A
provide an estimate of the 5-95 percentile range of possible trajectories.
While the actual trajectory that the world will follow is (hopefully)
statistically constrained by this range, there is no *a priori* reason why
it should be of a shape similar to the curves defining this range (for ex-
ample, a weighted mean of the 5-percentile minimum and 95-percentile
maximum limits). There is also no reason to suppose that plausible
trajectories could be constructed by taking independent random sam-
ples at a regular (e.g. annual) interval from frequency distributions
constrained by Tables I and II. A realistic trajectory would show some
limited variability about a smooth curve. Possible trajectories are there-
fore formed by first defining a set of ordered smooth curves (here called
courses), which are weighted averages of the 5-percentile minimum and
95-percentile maximum limits (see Fig. 2 for a schematic illustration).
Any given weighting and type of frequency distribution represents a
specific percentile value. The probability of a particular *course* being
realised is described by two plausible frequency distributions: normal
and uniform (or 'boxcar'). As is shown in Section 6, the results depend
only weakly on the chosen distribution. Each *course* is divided into
increments, the duration of which is here taken to be one year, which is
long enough to permit averaging over seasonal cycles but short enough
to allow appropriate resolution of the rising, and possibly accelerating,
sea level. It is also the time-scale over which interannual variability is
simulated, as described next.

Interannual variability, not accounted for by the present exceedance
distribution (see next paragraph), is represented by the addition of an
independent normally-distributed random perturbation (labelled $P_{i,k,l}$
in Fig. 2) to each of these *courses* each year (this is, of course, only a first
approximation to the true variability, which would exhibit significant
autocorrelation from year to year). The probability of mean sea level
having a certain value in any one year is therefore the combination of
the frequency distribution of the *courses* and the frequency distribution
describing the interannual variability. For the examples given in this pa-
per, this variability is prescribed to be zero, since the IPCC projections
give little guidance as to how it should be quantified, and any variabil-
ity introduced at this stage could lead to double-counting (because of

interannual variability included in the exceedance distribution based on recent historical data).

Annual maxima are derived from an observed sea-level ('tide gauge') record. A temporal trend of 1.1 mm/year is first removed from the record and the datum is adjusted so that the levels relate to the start of the base year (2000) of the projections (i.e. the data for the start of 2000 retains its original vertical datum during the detrending process). This trend is based on an Australian average rate of relative sea-level rise derived from Lambeck, 2002. Although the long-term trend has significant spatial variability, individual tidal records are often too short for its accurate local determination; an Australian average is therefore used here. Annual maxima are estimated using a clustering algorithm such that any extreme events closer than 3 days are counted as a single event, and any gaps in time are removed from the record. These annual maxima are then fitted to a *Generalized Extreme Value Distribution* (*GEV*) using the *ismev* package (Coles, 2001, pp. 54, 185) implemented in the statistical language *R* (R Development Core Team, 2008). This GEV distribution represents the 'present' (taken to be at the year 2000) AEP. The software estimates the maximum likelihood estimation of the exceedance distribution and its upper and lower 95-percentile confidence limits. These three 'distributions' (the quotes indicating that the envelopes of the upper and lower confidence limits are not, technically, statistical distributions in themselves) are used to make three independent estimates of the exceedance statistics for the prescribed future asset period, which are finally combined into a single exceedance distribution.

It should be noted that a GEV distribution has been used here mainly to provide an example of a suitable initial exceedance distribution. While the GEV distribution is reasonably robust and widely employed, there is no reason why other parametric or non-parametric distributions should not be used, so long as they provide an acceptable fit to the observed extremes. There are, indeed, clear examples of where a GEV distribution is not appropriate, such as locations which are infrequently impacted by surges induced by tropical cyclones. In such cases, the exceedance distribution often has significantly increased levels at the low-probability(or high-ARI) end, precluding any reasonable fit to a GEV distribution. Such an example is shown in Fig. 3, based on the century-long detrended sea-level record from Galveston, USA. The ARI has been here estimated by simply counting exceedances above each specific level, multiple exceedances which occur within a period of three days being counted as one. The vertical axis, here and in subsequent plots, has been labelled 'still water level' to indicate that none of the

results presented here includes the effects of waves (i.e. the results show changes in sea level after the waves have been removed).

Considering one of these three initial exceedance 'distributions' (shown schematically as $E_{i,1}$, $E_{i,2}$ and $E_{i,3}$ in Fig. 4), the exceedance distribution for each annual increment and each *course* is estimated by moving the present distribution upwards to describe the change in mean sea level and spreading it vertically to account for the prescribed interannual variability (assumed zero for the examples presented later). This process involves the convolution of the present exceedance statistics with the frequency distribution describing sea-level rise and its uncertainty. The exceedance distribution for the entire asset period for this *course* is then calculated by the sequential application of Eq. 2. The total exceedance distribution for the asset period is then derived by combining the exceedance distributions for each *course*, taking account of its inherent probability.

The above procedure yields three estimates of the exceedance distribution for the asset period: (1) based on the maximum likelihood estimate of the present annual exceedance distribution and (2) and (3) based on its upper and lower 95-percentile confidence limits. The final step is to make a small adjustment to (1) using the differences between (2) and (3) as indicators of the uncertainty in (1). This adjustment effectively yields a 'best estimate' of the exceedance distribution, taking into account its own uncertainty. The same adjustment is applied to the maximum likelihood estimate of the exceedance distribution at 2000 when presenting the results in Figs. 5 to 8.

6.   Results for Australia

Fig. 5 shows the result of the above analysis for Fremantle (southwestern Australia) for the (high) A1FI emission scenario and an asset period of 2010 to 2060 inclusive. The projections of sea-level rise used in this analysis include the contribution 'scaled-up ice sheet discharge' which represents land-ice processes which are at present poorly understood (Meehl et al., 2007, p. 820). In these analyses, which are for illustrative purposes only, the interannual variability in the projections (see Section 5) is set to zero, so that $P_{i,k,l}$ is given by Eq. (13) in Appendix B. It should however be noted that that some interannual variability is still included in this analysis by way of the present exceedance distribution. The red curves show the exceedance probabilities for 2010 to 2060 inclusive (the thick (middle) pair of curves are 'adjusted' maximum likelihood values, the outer pairs are the 95-percentile confidence limits and each pair corresponds to approximating the projection uncertainty

by normal and boxcar (uniform) distributions). The 'adjusted' maximum likelihood curves represent the best estimate of the exceedance distribution, taking into account its uncertainty (see Appendix B). It is evident that the choice of normal or boxcar distributions does not markedly affect the results. It should be noted that the vertical datum used here is present Mean Higher High Water (MHHW, defined here as mean sea level plus the sum of the amplitudes of the M_2, K_1 and O_1 tidal constituents (PCTMSL, 2007)) which, although being a fixed level (and hence robust datum) at a particular location, depends on the magnitude of the local tides and hence varies from place to place. However, the advantage of relating extremes to a 'high' tidal level such as MHHW, is that it removes much of the tidal variation from the result, so that the levels presented on the vertical axis of plots such as Fig. 5 are more likely to be applicable to nearby locations as well as to the location itself. The curves are terminated at the 'low-probability' end of the plot when the ARI estimated from historical records exceeds four times the record length, which represents a reasonable limit of extrapolation of the observations (Pugh, 1996). The blue curves in Fig. 5 show equivalent exceedance probabilities for an asset period of 51 years and mean sea level held constant at the 2000 value (the thick (middle) curve is the 'adjusted' maximum likelihood value and the outer curves are 95-percentile confidence limits).

It is important to distinguish between the three different types of vertical spread in Fig. 5. One involves the inherent uncertainty in the estimation of the present exceedance probability, which is indicated by the outer blue curves and by the outer pairs of red curves. The second involves the span of the exceedance probabilities themselves which represents the variability in the maximum sea levels observed over the asset period. A third contribution to the spread is the uncertainty in the projections of sea-level rise, as indicated by the minima and maxima in Tables I and II. This third contribution serves to increasingly widen the span of the exceedance probabilities for asset periods that are further into the future. However, in the case of Fig. 5, this latter effect is relatively small and the central red curves would fit closely with the central blue curve raised by the average increase of relative mean sea level from 2000 to the asset period (2010-2060 inclusive), which is about 0.1 m. This is an example where the vertical spread of the exceedance distribution for the asset period is dominated by the present (2000) exceedance distribution, and the uncertainty in the projections of mean sea level is relatively unimportant. In such cases it would be quite reasonable to allow for future sea-level rise by simply adding the projection of *mean* rise to the present exceedance distribution, without regard to the uncertainty of that rise. In other words, increasing a

planning level by the *maximum* projected rise would, in this instance, be overly conservative. Increasing a planning level by the mean projected rise is generally only valid for asset periods in the early part of the 21st century, during which time the uncertainty in projected sea-level rise is relatively small.

Fig. 6 shows an equivalent set of curves for Fort Denison (Sydney, southeastern Australia). Fort Denison has significantly larger tidal range (defined here as Mean Higher High Water - Mean Lower Low Water) than Fremantle (1.5 m compared with 0.6 m at Fremantle) and a smaller non-tidal variability (Church et al., 2006). It may seem surprising that a larger tidal range does not necessarily lead to an increased vertical spread of the exceedance distribution. However, this effect may be understood by considering the case of a sea-level time series composed of a single tidal harmonic, which has a flat exceedance distribution (i.e. one with no vertical spread) for any asset period which is long enough to contain at least one tidal cycle. The vertical spread of the exceedance distribution for Fort Denison is in fact smaller than the spread for Fremantle, the standard deviations of the corresponding frequency distributions being 0.05 m and 0.07 m at Fort Denison and Fremantle respectively. The uncertainty in the projections of mean sea level therefore has a more significant effect on the exceedance distribution at Fort Denison than at Fremantle, as is shown by the clearly detectable difference in slope between the central portions of the thick (middle) blue and red curves in Fig. 6 compared with Fig. 5.

Figs. 7 and 8 show equivalent exceedance distributions but for an asset period of 2010 to 2100 inclusive. For clarity, these figures have been simplified by omitting the 95-percentile confidence limits from both the present and future exceedance distributions. The remaining two curves for 2010-2100 (inclusive) correspond to approximating the projection uncertainty by normal and boxcar (uniform) distributions. Both figures now show the clear 'spreading' effect of the uncertainty in the projections of mean sea level, such that the central portion of the red curves (for 2010-2100 inclusive) is significantly steeper than the corresponding part of the blue curve. This raises an important implication for planning for later this century. If we are prepared to accept, say, an 80% probability of flooding of a particular piece of infrastructure at Fort Denison during the period 2010 to 2100 inclusive, then Fig. 8 indicates that planning levels should be raised by about 0.3 m relative to their 2000 levels (i.e. the difference between the blue and red curves for an exceedance probability of 0.8; see right-hand vertical arrow in Fig. 8). However, if we take a more precautionary approach and are only prepared to accept a 30% chance of flooding, the planning levels should be raised by about 0.45 m relative to their 2000 levels

(i.e. the difference between the blue and red curves for an exceedance probability of 0.3; see left-hand vertical arrow in Fig. 8); it should be noted that this is significantly larger than the average sea-level rise for this period of around 0.25 m. In other words, the amount by which planning levels need to be raised depends on the acceptable likelihood of flooding, diagrams like Figs. 5 to 8 providing a way of making the necessary choice. The technique may also be applied to sub-sets of the asset period in order to quantify the (increasing) likelihood of flooding as sea-level continues to rise during the 20th century.

7. Summary

The Fourth Assessment Report (IPCC, 2007b) has indicated a projected global sea-level rise of up to 0.79 metres in 2095 (relative to 1990) with the caveat that, because of uncertainties in future ice sheet flow, larger rises cannot be excluded.

A method of combining observations of present sea-level extremes with the (uncertain) projections of sea-level rise during the 21st century has been described, using Australian data as an example. The results provide engineers, planners and policymakers with a technique for estimating the probability that a given sea level will be exceeded during any prescribed period during this century, and therefore a way of choosing how planning levels should be raised to accommodate an acceptable likelihood of flooding.

Finally, it should be emphasised that the results and techniques presented in this paper relate only to the increase in the frequency of extremes caused by a rise in mean sea-level and not due to any additional increase in extremes *relative to* mean sea level, caused for example by more frequent and intense storminess. However, present evidence suggests that the rise in mean sea level is generally the dominant cause of the observed increase in the frequency of extreme events. The method may also be readily modified to accommodate future changes in the variability relative to mean sea level, once they are better understood.

Appendix

A. Proposed Time Series of Sea-Level Projections for the 21st Century

Both the IPCC TAR and the IPCC AR4 provide sea-level projections relative to 1990 (strictly, the AR4 provide them relative to the average

over 1980-1999). Unlike the IPCC TAR, the AR4 does not provide time series of sea-level projections through the 21st century, but only values for the decade 2090-2099 (here termed '2095'). For 2095, the TAR and AR4 projections agree well at the upper limit and rather worse at the lower limit. This Appendix suggests a way of adjusting the TAR time series so as to agree with the AR4 projections at 2095. Results are given for the six SRES 'marker' scenarios, A1B, A1T, A1FI, A2, B1 and B2. They are based on Table II.5 of the IPCC TAR (Church et al., 2001, pp. 824-825) and Table 10.7 of the IPCC AR4 (Meehl et al., 2007, p. 820).

The following procedure was employed:

1. Time series of the minima and maxima of the projections from 1990 to 2100, for the six SRES 'marker' scenarios, A1B, A1T, A1FI, A2, B1 and B2, were extracted from Table II.5 of the IPCC TAR (Church et al., 2001, pp. 824-825). The data were presented every decade. It should be noted that, for both the minima and maxima, the columns for A1T and A1FI were incorrectly placed in the IPCC TAR and were interchanged at this stage.

2. Values of minima and maxima for 2095 were obtained by averaging the 2090 and 2100 values in the tables obtained from (1).

3. Values of minima and maxima for 2095, for the six SRES 'marker' scenarios, were extracted from Table 10.7 of the IPCC AR4 (Meehl et al., 2007, p. 820), by adding the rows 'Sea level rise' and 'Scaled-up ice sheet discharge'. It should be noted that this does not exactly give the 0.79 m maximum sea-level rise at 2095 often quoted from the AR4, which approximates the row 'Scaled-up ice sheet discharge' by the range '0.1 to 0.2 m' (IPCC, 2007b; Meehl et al., 2007).

4. The ratios between the TAR and AR4 values at 2095 were calculated for the minima and maxima, for the six SRES 'marker' scenarios (from (2) and (3), respectively).

5. The time series for the minima and maxima, and for the six SRES 'marker' scenarios, from Table II.5 of the IPCC TAR, were multiplied by their respective ratios calculated in (4) . This yielded an adjusted version of Table II.5 of the IPCC TAR, which matches the AR4 projections at 2095.

The adjusted version of Table II.5 of the IPCC TAR is shown in Tables I and II, and in Fig. 1. Table II.5 also contained projections for the 'model average' but these cannot be used for generating an adjusted

time series because the AR4 did not provide numerical values for model average values at 2095.

The above analysis has a number of caveats and possible weaknesses:

1. The minima and maxima for the 'Sea level rise' and 'Scaled-up ice sheet discharge' in Table 10.7 of the IPCC AR4 have been added linearly, rather than in quadrature, implying that they are correlated (i.e. that the models which give higher 'sea level rise' also give more 'scaled-up ice sheet discharge'). Although this seems intuitively reasonable, it should be noted that the 'scaled-up ice sheet discharge' simply scales as the projected global-average temperature, and that there is no simple relationship between sea-level rise and global-average temperature – sea-level rise depends, to a large extent, on the integral of past global-average temperature (e.g. Rahmstorf, 2007). However, it should be noted that, when the uncertainties in Table 10.7 of the IPCC AR4 were accumulated, it was assumed that the uncertainties in global temperature and thermal expansion were correlated; since the sea-level rise projections during the 21st century are dominated by thermal expansion, this adds support to the assumption that global temperature, 'sea level rise' and 'scaled-up ice sheet discharge' are correlated when uncertainties are accumulated.

2. There are clear differences between the meaning of the range of projections for the TAR and AR4:

   a) For the TAR, they are 'the range of all AOGCMs *(Atmosphere-Ocean General Circulation Models – i.e. climate models)* . . . including uncertainty in land-ice changes, permafrost changes and sediment deposition'. On the assumption that the range of the projections is primarily the range of simulations from the various climate models, an estimate may be made of the standard deviation of the distribution of the projections. If the climate models are assumed to be independent, then the number of degrees of freedom associated with the TAR projections is probably around ten, since these results were based on seven climate models and a few additional estimates (e.g. for ice melt). From elementary order statistics, it may be estimated that the range of TAR projections (i.e. the largest projection minus the smallest) is approximately $\mu \pm 1.5\sigma$ where μ and σ are the mean and standard deviation of the statistical distribution from which the particular models projections have been drawn. However, it should be noted that the mean and standard deviation describe the *distribution of possible projections* and not the *uncertainty*

in the best estimate of the projection (to confuse these is equiv-
alent to confusing the standard deviation with the standard
error).

b) For the AR4, they are the '5 to 95% range' (equivalent to $\mu \pm 1.64\sigma$), which presumably relates to the uncertainty in the best
estimate of the projection and *not* to the distribution of possible
projections.

3. As indicated in 2(a) and 2(b), above, the issue of whether the
IPCC projections represent *distribution of possible projections* or
the *uncertainty in the best estimate of the projection* needs to be
considered. Since the number of degrees of freedom (which could be
somewhat larger than the number of contributing climate models)
is of order ten, the standard deviation and standard error could
differ by a factor of at least three.

B. Method of Estimating Future Exceedance Probability

The method is here presented in discrete form so as to facilitate the
development of equivalent numerical algorithms.

It should be noted that the sea-level rise projections used in the
following should represent the *relative* local sea-level rise (i.e. the sea-
level rise relative to the local land surface). These would most easily
be derived from the global AR4 projections (see Appendix A) with ap-
propriate adjustments for vertical land motion and any known regional
variations.

The annual exceedance distribution would normally be derived from
an observational (tide gauge) or modelled relative sea-level record. Prior
to use, any temporal trend should be removed from the record and the
datum adjusted so that the levels relate to the base year (y_0 in the
following analysis).

Two interlaced vertical grids are defined:

$$z_E = z_0 + i\delta z \qquad (4)$$

and

$$z_F = z_0 + \left(i + \frac{1}{2}\right)\delta z \qquad (5)$$

where z_E, z_F and z_0 are vertical coordinates, i is an integer and δz is
the discretisation interval. z_E and z_F are the coordinates for exceedance
and frequency distributions, respectively. z_0 is a constant offset, the

vertical coordinate for an exceedance distribution when $i = 0$. The coordinates are interlaced in this way so that a simple rectangular integration approximation may be used to convert frequency distributions to exceedance distributions (see below).

Time is defined by the index, k, and year, y, given by:

$$y = y_0 + k \tag{6}$$

where y_0 is the year for which $k = 0$.

The exceedance distribution of annual maxima (the 'annual exceedance distribution'), E, and the corresponding frequency distribution, F, for year y_0 (i.e. $k = 0$), are related by (using the rectangular integration approximation):

$$E_{i,j} = \delta z \sum_{m=i}^{\infty} F_{m,j} \tag{7}$$

and

$$F_{i,j} = \frac{E_{i,j} - E_{i+1,j}}{\delta z} \tag{8}$$

where i is the index of the level (Eqs.(4) and (5)).

The index j denotes the 95-percentile lower limit ($j = 1$), the maximum likelihood estimate ($j = 2$) and the 95-percentile upper limit ($j = 3$). The following analysis is performed separately using ($j = 1, 2, 3$), the results being finally combined at the end to give a best estimate of the total exceedance probability. These distributions are shown schematically in Fig. 4.

The annual mean sea level rise (relative to year y_0) and its corresponding probability is described by the frequency distribution, $P_{i,k,l}$, where i represents the vertical coordinate, k represents the year and l represents the particular sea-level rise *course* (see Fig. 2).

The vertical coordinate, z_P, for $P_{i,k,l}$ is defined by:

$$z_P = i\delta z \tag{9}$$

which is measured relative to mean sea level at $k = 0$ or year y_0.

The annual mean sea level rise for the year with index k, and for the *course l*, is given by:

$$R_{k,l} = \delta z \sum_{i=-\infty}^{\infty} z_P P_{i,k,l} = (\delta z)^2 \sum_{i=-\infty}^{\infty} i P_{i,k,l} \tag{10}$$

which is prescribed by taking a weighted mean of the available IPCC 5-percentile minimum and 95-percentile maximum projection limits, $z_{k,5}$ and $z_{k,95}$:

$$R_{k,l} = w_l z_{k,5} + (1 - w_l) z_{k,95} \tag{11}$$

where w_l is a weight which is constant for each *course*, l, and is chosen as described below.

For year y_0:

$$P_{i,0,l} = \frac{1}{\delta z} \quad \text{for} \quad i = 0 \quad \text{otherwise} \quad 0 \tag{12}$$

For year $y_0 + k$ and the special case of $P_{i,k,l}$ having no spread in i, a sea-level rise of $i'\delta z$ (relative to year y_0) is described by:

$$P_{i,k,l} = \frac{1}{\delta z} \quad \text{for} \quad i = i' \quad \text{otherwise} \quad 0 \tag{13}$$

which is a Dirac delta function centred on $i = i'$.

A general distribution, $P_{i,k,l}$, and its relationship to the *course*, l, is shown schematically in Fig. 2.

In practice, the vertical discretisation is chosen such that the range of i included in the sums in Eq. (10) may be truncated to $[i_{min}, i_{max}]$ without appreciable loss of accuracy.

The sea-level rise *course* l is assumed to have a probability of occurrence Q_l, where:

$$\sum_{1}^{l_{max}} Q_l = 1 \tag{14}$$

Q_l and w_l are chosen so as to be consistent with the particular distribution (normal or uniform) chosen for the projection uncertainties. For the examples shown in Figs. 5 to 8, Q_l was a constant, independent of l.

The technique now proceeds, as follows, with the convolution (Eq. 15) of $F_{i,j}$ (Fig. 4) with $P_{i,k,l}$ (Fig. 2), combining the results over the *asset period* (a prescribed range of k; Eq. 17) and over all *courses*, l, (Eq. 18) to yield the projected exceedance distribution.

With the inclusion of sea-level rise, the frequency distribution of annual maxima for the year with index k is given by:

$$F'_{i,j,k,l} = \delta z \sum_{m=-\infty}^{\infty} F_{i-m,j} P_{m,k,l} \quad j = 1, 2, 3 \tag{15}$$

which has an equivalent exceedance distribution given by:

$$E'_{i,j,k,l} = \delta z \sum_{m=i}^{\infty} F'_{m,j,k,l} \quad j = 1, 2, 3 \tag{16}$$

(using a similar relationship to Eq. 7).

If it is assumed that the variability defined by $P_{i,k,l}$ (and hence the variability inherent in $F'_{i,j,k,l}$ and $E'_{i,j,k,l}$) is statistically independent between years, then for a period covering the years with index range $[k_1, k_2]$, the exceedance probability is given by (using Eq. 2):

$$E''_{i,j,k_1,k_2,l} = 1 - \prod_{k=k_1}^{k_2} (1 - E'_{i,j,k,l}) \qquad j = 1, 2, 3 \qquad (17)$$

The total exceedance probability, covering all courses is therefore given by:

$$E'''_{i,j,k_1,k_2} = \sum_{l=1}^{l_{max}} E''_{i,j,k_1,k_2,l} Q_l \qquad j = 1, 2, 3 \qquad (18)$$

which has an equivalent frequency distribution given by:

$$F'''_{i,j,k_1,k_2} = \frac{E'''_{i,j,k_1,k_2} - E'''_{i+1,j,k_1,k_2}}{\delta z} \qquad j = 1, 2, 3 \qquad (19)$$

The uncertainty inherent in E'''_{i,j,k_1,k_2} and F'''_{i,j,k_1,k_2} may be inferred from the differences of E'''_{i,j,k_1,k_2} for $j = 1, 2, 3$ (which have been derived from the 95-percentile lower limit $(E_{i,1})$, the maximum likelihood estimate $(E_{i,2})$ and the 95-percentile upper limit $(E_{i,3})$ of the present annual exceedance distribution). An adjusted frequency distribution, F''''_{i,k_1,k_2}, taking account of this uncertainty, may be derived by convolving $F'''_{i,2,k_1,k_2}$ (the total exceedance probability, based on the maximum likelihood estimate of the annual exceedance, $E_{i,2}$), with a kernel S_m which has a standard deviation s and a form equivalent to that of the uncertainty distribution:

$$F''''_{i,k_1,k_2} = \delta z \sum_{m=-\infty}^{\infty} F'''_{i-m,2,k_1,k_2} S_m \qquad (20)$$

which has an equivalent exceedance distribution given by:

$$E''''_{i,k_1,k_2} = \delta z \sum_{m=i}^{\infty} F''''_{i,k_1,k_2} \qquad (21)$$

E''''_{i,k_1,k_2} is the appropriate exceedance distribution which describes exceedances over the period covering the years with index range $[k_1, k_2]$, taking into account the uncertainty in the estimate of E'''_{i,j,k_1,k_2}. However, in practice, because the standard deviation in $F'''_{i,2,k_1,k_2}$ is typically five times larger than s, $E''''_{i,k_1,k_2} \approx E'''_{i,2,k_1,k_2}$. For the present work, s is

estimated from the difference between $E'''_{i,1,k_1,k_2}$ and $E'''_{i,3,k_1,k_2}$, assuming that S_m is a normal distribution.

Acknowledgements

References

Bindoff, N., J. Willebrand, V. Artale, A. Cazenave, J. Gregory, S. Gulev, K. Hanawa, C. L. Quéré, S. Levitus, Y. Nojiri, C. Shum, L. Talley, and A. Unnikrishnan: 2007, *Climate Change 2007: The Physical Science Basis. Contribution of Working Group I to the Fourth Assessment Report of the Intergovernmental Panel on Climate Change*, Chapt. 5, pp. 385–432. Cambridge, United Kingdom and New York, NY, USA: Cambridge University Press.

Canadell, J., C. L. Quéré, M. Raupach, C. Field, E. Buitenhuis, P. Ciais, T. Conway, N. Gillett, R. Houghton, and G. Marland: 2007, 'Contributions to accelerating atmospheric CO_2 growth from economic activity, carbon intensity, and efficiency of natural sinks'. *Proceedings of the National Academy of Sciences* **104**, 18866–18870.

Church, J., J. Gregory, P. Huybrechts, M. Kuhn, K. Lambeck, M. Nhuan, D. Qin, and P. Woodworth: 2001, *Climate Change 2001: The Scientific Basis, Contribution of Working Group 1 to the Third Assessment Report of the Intergovernmental Panel on Climate Change*, Chapt. 11, pp. 639–693. Cambridge, United Kingdom and New York, NY, USA: Cambridge University Press.

Church, J., J. Hunter, K. McInnes, and N. White: 2006, 'Sea-level rise around the Australian coastline and the changing frequency of extreme sea-level events'. *Australian Meteorological Magazine* **55**, 253–260.

Church, J. and N. White: 2006, 'A 20th century acceleration in global sea-level rise'. *Geophysical Research Letters* **33**(L01602), doi:10.1029/2005GL024826.

Church, J., N. White, T. Aarup, W. Wilson, P. Woodworth, C. Domingues, J. Hunter, and K. Lambeck: 2008, 'Understanding global sea levels: past, present and future'. *Sustainability Science* **3**(1), 9–22.

Coles, S.: 2001, *An Introduction to Statistical Modeling of Extreme Values*. London, Berlin, Heidelberg: Springer-Verlag.

Grinsted, A., J. Moore, and S. Jevrejeva: 2009, 'Reconstructing sea level from paleo and projected temperatures 200 to 2100 AD'. *Climate Dynamics* pp. doi:10.1007/s00382–008–0507–2.

Hansen, J.: 2007, 'Scientific reticence and sea level rise'. *Environmental Research Letters* **2**(024002), doi:10.1088/1748–9326/2/2/024002.

Holgate, S., S. Jevrejeva, P. Woodworth, and S. Brewer: 2007, 'Comment on 'A Semi-Empirical Approach to Projecting Future Sea-Level Rise''. *Science* **317**(5846), 1866b–1866c, doi:10.1126/science.1140942.

Holgate, S. and P. Woodworth: 2004, 'Evidence for enhanced coastal sea level rise during the 1990s'. *Geophysical Research Letters* **31**(L07305), doi:10.1029/2004GL019626.

Horton, R., C. Herweijer, C. Rosenzweig, J. Liu, V. Gornitz, and A. Ruane: 2008, 'Sea level rise projections for current generation CGCMs based on the semi-empirical method'. *Geophysical Research Letters* **35**(L02715), doi:10.1029/2007GL032486.

IPCC: 2007a, *Climate Change 2007: The Physical Science Basis. Contribution of Working Group I to the Fourth Assessment Report of the Intergovernmental Panel on Climate Change.* Cambridge, United Kingdom and New York, NY, USA: Cambridge University Press.

IPCC: 2007b, *Climate Change 2007: The Physical Science Basis. Contribution of Working Group I to the Fourth Assessment Report of the Intergovernmental Panel on Climate Change, Summary for Policymakers.* Cambridge, United Kingdom and New York, NY, USA: Cambridge University Press.

Jevrejeva, S., A. Grinsted, J. Moore, and S. Holgate: 2006, 'Nonlinear trends and multiyear cycles in sea level records'. *Journal of Geophysical Research* **111**(C09012), doi:10.1029/2005JC003229.

Lambeck, K.: 2002, 'Sea level change from mid Holocene to recent time: an Australian example with global implications'. In: *Ice Sheets, Sea Level and the Dynamic Earth*, Vol. 29 of *Geodynamics Series.* American Geophysical Union, pp. 33–50.

Lemke, P., J. Ren, R. Alley, I. Allison, J. Carrasco, G. Flato, Y. Fujii, G. Kaser, P. Mote, R. Thomas, and T. Zhang: 2007, *Climate Change 2007: The Physical Science Basis. Contribution of Working Group I to the Fourth Assessment Report of the Intergovernmental Panel on Climate Change*, Chapt. 4, pp. 337–383. Cambridge, United Kingdom and New York, NY, USA: Cambridge University Press.

Meehl, G., T. Stocker, W. Collins, P. Friedlingstein, A. Gaye, J. Gregory, A. Kitoh, R. Knutti, J. Murphy, A. Noda, S. Raper, I. Watterson, A. Weaver, and Z.-C. Zhao: 2007, *Climate Change 2007: The Physical Science Basis. Contribution of Working Group I to the Fourth Assessment Report of the Intergovernmental Panel on Climate Change*, Chapt. 10, pp. 747–845. Cambridge, United Kingdom and New York, NY, USA: Cambridge University Press.

PCTMSL: 2007, *Australian Tides Manual, Special Publication No. 9.* Permanent Committee on Tides and Mean Sea Level, Commonwealth of Australia, http://www.icsm.gov.au/tides/SP9/sp9.pdf.

Pfeffer, W., J. Harper, and S. O'Neel: 2008, 'Kinematic constraints on glacier contributions to 21st-century sea-level rise'. *Science* **321**(5894), 1340–1343, doi:10.1126/science.1159099.

Pugh, D.: 1996, *Tides, Surges and Mean Sea-Level.* Chichester, New York, Brisbane, Toronto and Singapore: John Wiley & Sons, reprinted with corrections, http://eprints.soton.ac.uk/19157/01/sea-level.pdf.

R Development Core Team: 2008, 'R: A Language and Environment for Statistical Computing'. R Foundation for Statistical Computing, Vienna, Austria. ISBN 3-900051-07-0.

Rahmstorf, S.: 2007, 'A semi-empirical approach to projecting future sea-level rise'. *Science* **315**(5810), 368–370.

Rahmstorf, S., A. Cazenave, J. Church, J. Hansen, R. Keeling, D. Parker, and R. Somerville: 2007, 'Recent climate observations compared to projections'. *Science* **316**(5825), 709.

Raupach, M., G. Marland, P. Ciais, C. L. Quéré, J. Canadell, G. Klepper, and C. Field: 2007, 'Global and regional drivers of accelerating CO_2 emissions'. *Proceedings of the National Academy of Sciences* **104**, 10288–10293.

Schmith, T., S. Johansen, and P. Thejll: 2007, 'Comment on 'A semi-empirical approach to projecting future sea-level rise''. *Science* **317**(5846), 1866c, doi:10.1126/science.1143286.

Woodworth, P. and D. Blackman: 2004, 'Evidence for systematic changes in extreme high waters since the mid-1970s'. *Journal of Climate* **17**(6), 1190–1197.

Woodworth, P., N. White, S. Jevrejeva, S. Holgate, J. Church, and W. Gehrels: 2008, 'Evidence for the accelerations of sea level on multi-decade and century timescales'. *International Journal of Climatology* **29**, 777–789, doi:10.1002/joc.1771.

Table I. Adjusted projections of sea-level (mm) for 5-percentile minima, derived by adjusting the TAR projections to correspond with the AR4 projections at 2095.

Year	A1B	A1T	A1FI	A2	B1	B2
1990	0	0	0	0	0	0
2000	10	11	9	9	12	11
2010	21	23	19	20	26	24
2020	35	42	32	32	44	42
2030	55	63	48	47	64	63
2040	77	86	69	67	84	83
2050	102	112	96	89	105	103
2060	126	135	130	115	127	125
2070	150	156	165	142	145	146
2080	173	173	200	173	161	168
2090	192	186	234	203	175	190
2100	208	194	266	237	185	210

Table II. Adjusted projections of sea-level (mm) for 95-percentile maxima, derived by adjusting the TAR projections to correspond with the AR4 projections at 2095.

Year	A1B	A1T	A1FI	A2	B1	B2
1990	0	0	0	0	0	0
2000	27	26	28	27	25	26
2010	59	59	60	60	56	58
2020	96	100	99	97	92	97
2030	143	149	146	139	132	142
2040	200	208	204	190	178	192
2050	266	272	278	251	227	247
2060	337	342	368	320	279	307
2070	413	413	471	401	333	369
2080	493	482	584	490	388	435
2090	571	548	701	588	444	504
2100	649	611	819	692	496	576
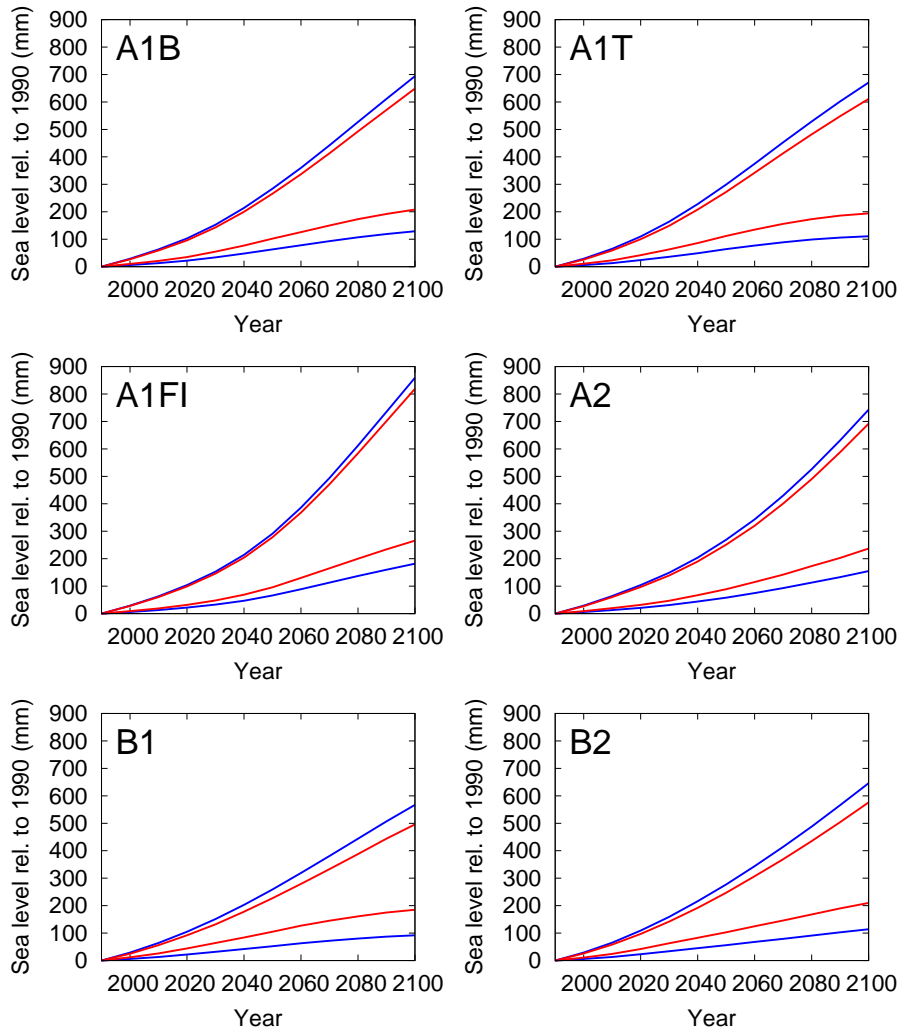
Figure 1. Adjusted projections of sea-level (mm, red), derived by adjusting the TAR projections (blue) to correspond with the AR4 projections at 2095. The upper and lower blue curves show the full range of the TAR projections. The upper and lower red curves are 5-percentile minima and 95-percentile maxima, respectively.
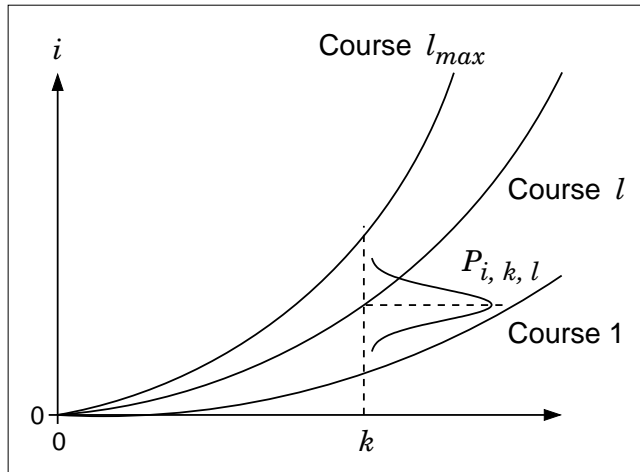
Figure 2. Schematic showing the way in which a given *course*, l, and associated interannual variability are related to the frequency distribution, $P_{i,k,l}$. The vertical axis (i) is the index for the sea level discretisation and sea level is $i\delta z$. The horizontal axis (k) represents time in years. The levels are proportional to i as defined by Eq. (9). The frequency distribution, $P_{i,k,l}$ is shown for the year $y_0 + k$ and for the *course l*. The mean of $P_{i,k,l}$ over i coincides with the *course l* at the year $y_0 + k$. The spread of $P_{i,k,l}$ in i represents interannual variability not accounted for by the exceedance distribution $E_{i,j}$. In the examples shown in Figs. 5 to 8 this spread is zero and $P_{i,k,l}$ is a Dirac delta function located on the *course l* at the year $y_0 + k$.
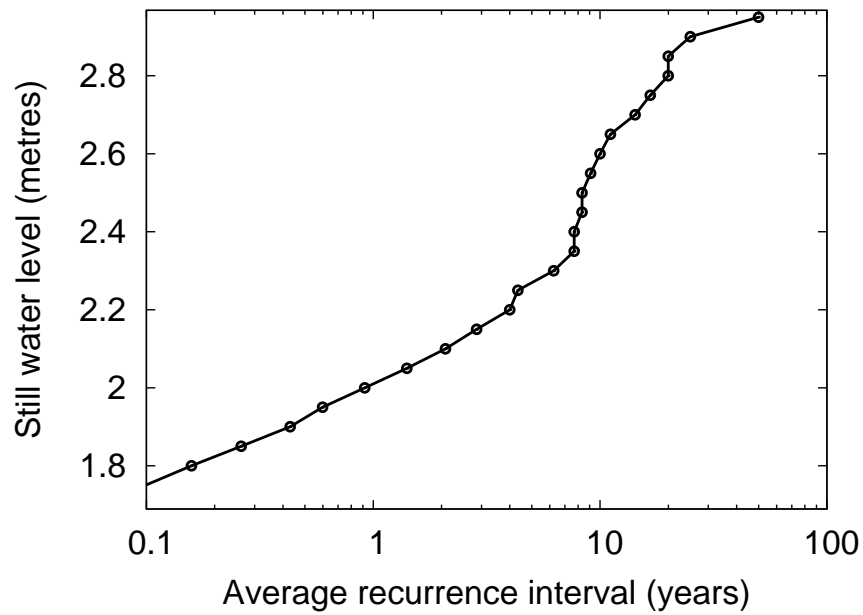
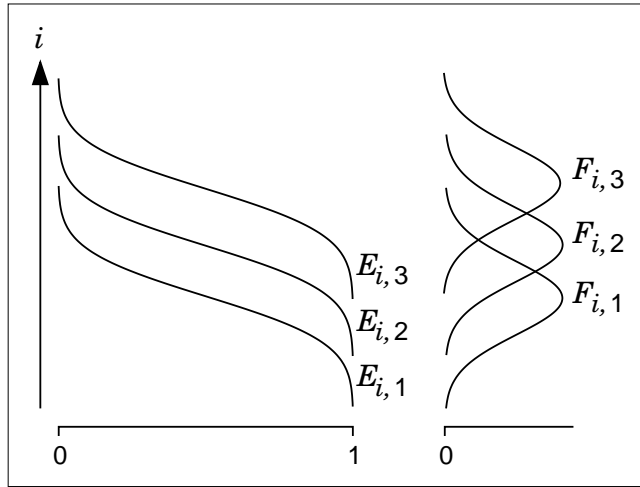*Figure 3.* Average recurrence interval for Galveston, USA, based on sea-level data from 1904 to 2006.

Figure 4. Schematic showing the annual exceedance distribution, $E_{i,j}$, and equivalent frequency distribution of annual maxima, $F_{i,j}$, of sea level at the base year, y_0 ($k = 0$). The levels are proportional to i as defined by Eqs. (4) and (5). The vertical axis (i) is the index for the sea level discretisation and sea level is $i\delta z$. The horizontal axes are probabilities. Three exceedance ($E_{i,j}$) and frequency ($F_{i,j}$) distributions are shown, corresponding to the 95-percentile lower limit ($k = 1$), the maximum likelihood estimate ($k = 2$) and the 95-percentile upper limit ($k = 3$).
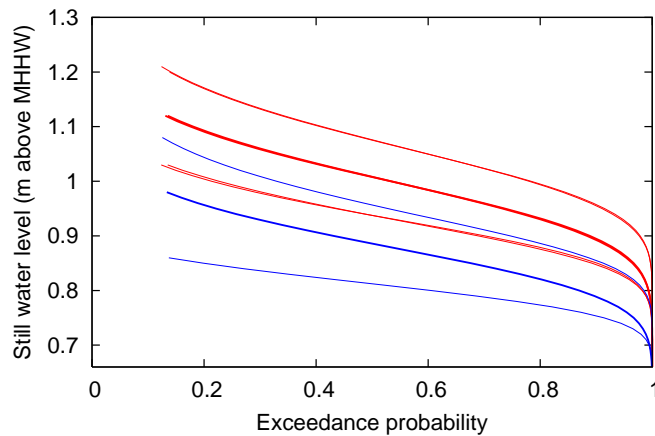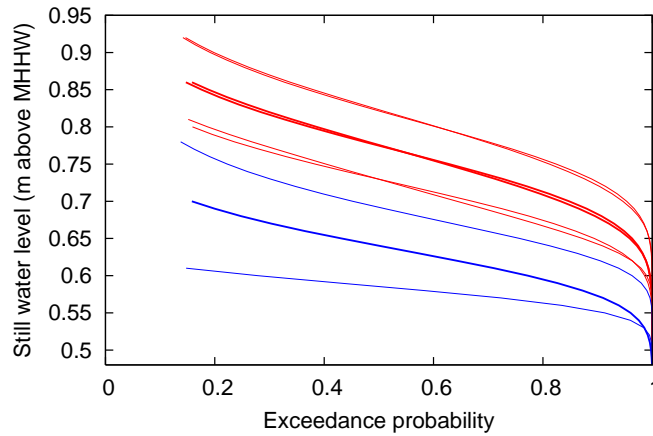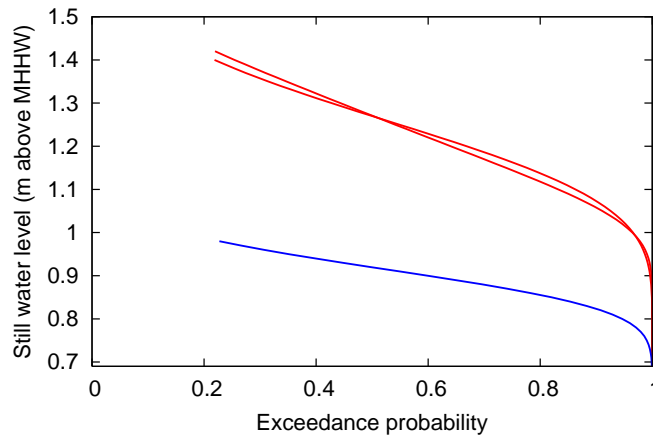

Figure 5. Exceedance probabilities for Fremantle, emission scenario A1FI, for an asset period of 2010 to 2060 inclusive (red; thick (middle) pair of curves represents 'adjusted' maximum likelihood values, outer pairs are 95-percentile confidence limits; each pair corresponds to approximating the projection uncertainty by normal and boxcar (uniform) distributions). Also shown are equivalent exceedance probabilities for an asset period of 51 years and mean sea level held constant at the 2000 value (blue; middle curve is 'adjusted' maximum likelihood value, outer curves are 95-percentile confidence limits). The 'adjusted' maximum likelihood curves represent the best estimate of the exceedance distribution, taking into account its uncertainty. Note that the pairs of red curves associated with normal and boxcar distributions are not always clearly distinguishable.

Figure 6. Exceedance probabilities for Fort Denison (Sydney), emission scenario A1FI, for an asset period of 2010 to 2060 inclusive (red; thick (middle) pair of curves represents 'adjusted' maximum likelihood values, outer pairs are 95-percentile confidence limits; each pair corresponds to approximating the projection uncertainty by normal and boxcar (uniform) distributions). Also shown are equivalent exceedance probabilities for an asset period of 51 years and mean sea level held constant at the 2000 value (blue; middle curve is 'adjusted' maximum likelihood value, outer curves are 95-percentile confidence limits). The 'adjusted' maximum likelihood curves represent the best estimate of the exceedance distribution, taking into account its uncertainty. Note that the pairs of red curves associated with normal and boxcar distributions are not always clearly distinguishable.

Figure 7. Exceedance probabilities for Fremantle, emission scenario A1FI, for an asset period of 2010 to 2100 inclusive (red; the two curves represent 'adjusted' maximum likelihood values corresponding to approximating the projection uncertainty by normal and boxcar (uniform) distributions). Also shown are equivalent exceedance probabilities for an asset period of 91 years and mean sea level held constant at the 2000 value (blue; curve is 'adjusted' maximum likelihood value). The 'adjusted' maximum likelihood curves represent the best estimate of the exceedance distribution, taking into account its uncertainty.
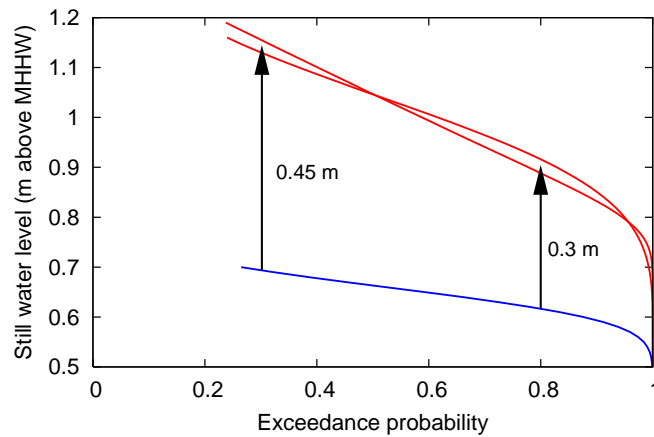
Figure 8. Exceedance probabilities for Fort Denison (Sydney), emission scenario A1FI, for an asset period of 2010 to 2100 inclusive (red; the two curves represent 'adjusted' maximum likelihood values corresponding to approximating the projection uncertainty by normal and boxcar (uniform) distributions). Also shown are equivalent exceedance probabilities for an asset period of 91 years and mean sea level held constant at the 2000 value (blue; curve is 'adjusted' maximum likelihood value). The 'adjusted' maximum likelihood curves represent the best estimate of the exceedance distribution, taking into account its uncertainty. Vertical arrows indicate amount that planning levels should be raised to cater for 80% and 30% likelihood of flooding.